

Electrochemically Modulated Diffraction

A Novel Strategy for the Determination of Conduction-Band-Edge Energies for Nanocrystalline Thin-Film Semiconductor Electrodes

Xiaojun Dang, Aaron M. Massari,* and Joseph T. Hupp**^z

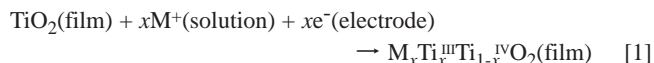
Department of Chemistry and Institute for Environmental Catalysis, Northwestern University, Evanston, Illinois 60208, USA

Micropatterned titanium dioxide thin-film electrodes exhibit efficient diffraction in the presence of aqueous or nonaqueous electrolyte solutions. The diffraction efficiency can be modulated electrochemically. At the wavelengths examined, the modulation is caused by changes in both real and imaginary components of the refractive index. The index changes, in turn, are caused by the addition of electrons to near-band-edge trap sites and by optical absorption by the trapped electrons. The onset potential for diffraction modulation provides a good measure of the potential of the electrode's conduction bandedge. Variable excitation wavelength measurements show that, after correction for absorption losses, the electrochemically induced changes in the proportion of light diffracted can be either positive or negative. The signs and the relative magnitudes of the wavelength-dependent changes are well described by a Kramers-Kronig analysis that assumes that changes in the real component of the refractive index dominate the response.

© 2000 The Electrochemical Society. S1099-0062(00)07-101-7. All rights reserved.

Manuscript received July 25, 2000. Available electronically October 2, 2000.

High area, thin-film metal oxide semiconductors have recently attracted tremendous attention in the electrochemical and photoelectrochemical community because of their potential utilities in photo-voltaic,^{1,2} photocatalytic,^{3,4} electrochromic,⁵ and battery⁶ applications. The success of these applications relies to a significant extent on understanding the chemical and physical factors that define the energetics of the interface, including band-edge energetics. Conduction-band-edge energy (E_{cb}) assessment via traditional electrochemical impedance methods and related methods is often considered problematic for high porosity, nanocrystalline semiconducting materials.⁷ The problems stem, in part, from the nonidealities introduced in impedance responses by high surface area electrode configurations. They also stem from the inability to establish appreciable potential drops across the space-charge layers of moderately doped, nanometer scale electrode particles.⁸ Fitzmaurice and co-workers developed spectroelectrochemical techniques to estimate E_{cb} values for nanocrystalline titanium dioxide electrodes by optically monitoring the appearance of electrons associated with near-band-edge trap sites.⁹ A reflectance strategy, which relied upon attenuation of reflected (rather than transmitted) near-infrared light, has also been reported.¹⁰ Electrochemical quartz crystal microgravity (EQCM)^{11,12} has also been used to assess conduction-band-edge energies for semiconducting metal oxide electrodes (TiO_2 , SnO_2 , ZnO_2 , ZrO_2). The EQCM studies have additionally shown that the addition of electrons to near-band-edge traps is accompanied by cation uptake; protons in the case of water, small electrolyte cations in the case of nonhydroxylic solvents.¹³ For example



Furthermore, it has recently been shown that coupled proton uptake and electron trapping processes can account for the extended Nernstian dependence of E_{cb} for nanocrystalline titanium dioxide on pH (*i.e.*, *ca.* -60 mV per pH unit variation over a *ca.* 30 pH unit range).^{11,14}

In this paper, we describe visible and near-infrared region transmissive optical diffraction studies of semiconductor-electrode/solution interfaces. Specifically, transparent conductive platforms modified with microscopically patterned titanium dioxide (anatase) thin

films have been examined as optical gratings. The periodicity of the semiconductor microarray and the existence of a higher refractive index for the semiconductor ($n = 2.7$) than for the electrolyte solution filling periodic gaps ($n = 1.3$ - 1.4) in the array lead to efficient and visually observable diffraction of coherent light (laser light) of wavelength comparable to the gap spacing. Manipulation of the electrode potential in the vicinity of the conduction bandedge leads to reversible changes in the diffraction efficiency. Depending on the wavelength of the incident light, the proportion of transmitted light that is diffracted can either increase or decrease upon potential-controlled addition of electrons to the semiconductor. The effects can be qualitatively explained via a simple Kramers-Kronig analysis of the electrode's light-absorption properties. The diffraction modulation effect has been used to assess E_{cb} for nanocrystalline anatase in contact with Li^+ -containing propylene carbonate solutions, and with a series of aqueous electrolyte solutions spanning a comparatively wide range of pH values. The values obtained are in good agreement with those reported in the literature.

Experimental

Preparation of patterned TiO_2 films.—Patterned polydimethylsiloxane (PDMS) stamps for microtransfer molding were fabricated according to a previously described method.¹⁵ The individual stamp feature size was $5 \times 5 \mu\text{m}$ (lateral) with a depth of 180 nm. The PDMS stamps were inked with a thermally curable epoxy (TRACON F114) and were then placed on a clean conductive indium tin oxide (ITO) platform. The ITO/epoxy/PDMS mold was cured at 60°C for 1 h and a patterned ITO platform was obtained.

Electrodeposition of TiO_2 on patterned ITO platforms was carried out in 50 mM TiCl_3 aqueous solution (pH 2.5).¹⁶ The epoxy patterned ITO platform acted as working electrode with a 2.2 cm^2 area exposed to the electrolyte solution. Suitable TiO_2 thin films were obtained after ~20 min by applying a fixed potential (0.04 V vs. Ag/AgCl reference electrode). The resulting films were carefully washed with water, dried at room temperature, and annealed in air at 450°C for 1 h to yield patterned films, which were found via X-ray powder diffraction measurements to be the anatase form of TiO_2 .

Diffraction measurements.—Light sources for diffraction were He-Ne lasers (543 and 633 nm), a diode laser (834 nm), and a Nd:yttrium aluminum garnet (YAG) laser (1064 nm), each configured normal to the surface of the ITO-supported TiO_2 grating. The grating film, acting as the working electrode, was held in electrolyte solution in a quartz cell containing an Ag/AgCl reference electrode

* Electrochemical Society Student Member.

** Electrochemical Society Active Member.

^z E-mail: jthupp@chem.nwu.edu

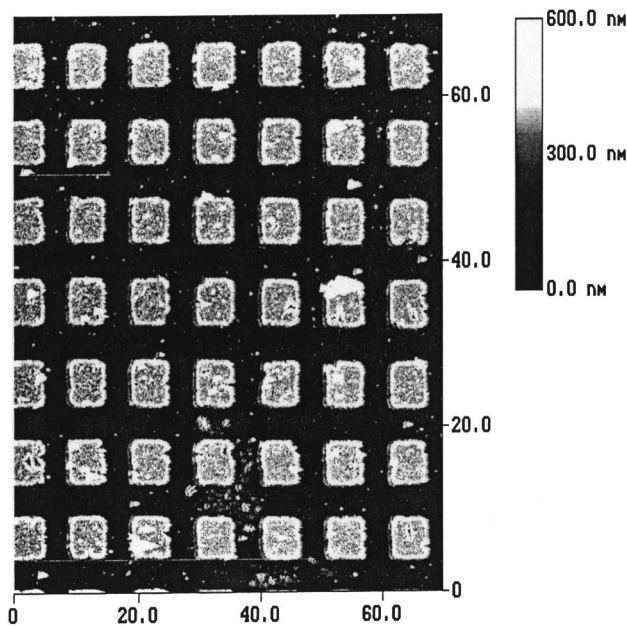


Figure 1. A $70 \times 70 \mu\text{m}$ AFM height image of a patterned TiO_2 thin film on ITO prepared via microtransfer molding and electrochemical deposition methods. The individual feature size was $5 \times 5 \mu\text{m}$ (lateral) with a height of $\sim 115 \text{ nm}$.

and a Pt wire counter electrode. All potentials are reported vs. Ag/AgCl. Potentials were controlled with a BAS potentiostat (model CV-27). The intensities of the undiffracted center beam (I_{00}) and one of the first-order diffraction beams (I_{10} or I_{11}) were monitored with photodiodes. The experimental data were collected using a personal computer via an in-house module written with Labview software (National Instruments Corp., Austin, TX). Control of solution pH was achieved with 0.05 M solutions of potassium chloride/hydrochloric acid (pH 1-2), potassium biphthalate (pH 4), potassium phosphonate monobasic/sodium hydroxide (pH 5-8) and potassium carbonate/potassium borate/potassium hydroxide (pH 10). For highly acid solutions ($H_0 = -1.05$) the electrolyte was 3.0 M HCl.¹⁷

Results and Discussion

Potential-modulated diffraction in a nonhydroxylic solution.—A representative atomic force microscopy (AFM) image of a patterned TiO_2 thin film is shown in Fig. 1. The image was obtained in tapping mode with a single etched silicon (TESP) nanoprobe SPM tip. The regularity of this array was maintained over $\sim 25 \text{ mm}^2$ ($\sim 33,000$ squares). The average film thickness in the area examined was 115 nm.

Passage of coherent, monochromatic, visible-region light through a patterned TiO_2 film yields an intense 2-D diffraction pattern. The diffraction efficiency (η), defined as the ratio of total diffracted light intensity (I_{diff}) to incident light intensity (I_{inc}), can be modulated by changing the applied potential. Figure 2 illustrates data acquired during an experiment where diffraction was monitored while the electrode potential was stepped from 0 to -1.2 V in -0.2 V increment in 1 M LiClO_4 /propylene carbonate solution. Significant reversible decreases in first-order diffraction efficiency are observed, beginning at -0.6 V , with greater decreases at more negative potentials. To probe the process further, a potential scanning experiment, with a scan rate of 1 mV/s , was performed between 0 and -1.2 V . The experiment yielded decreases in diffraction efficiency, with an onset potential of $\sim -0.6 \text{ V}$ (data not shown).

Notably, the onset potential is reasonably close to the potential typically reported for the conduction bandedge in this solvent.¹⁸

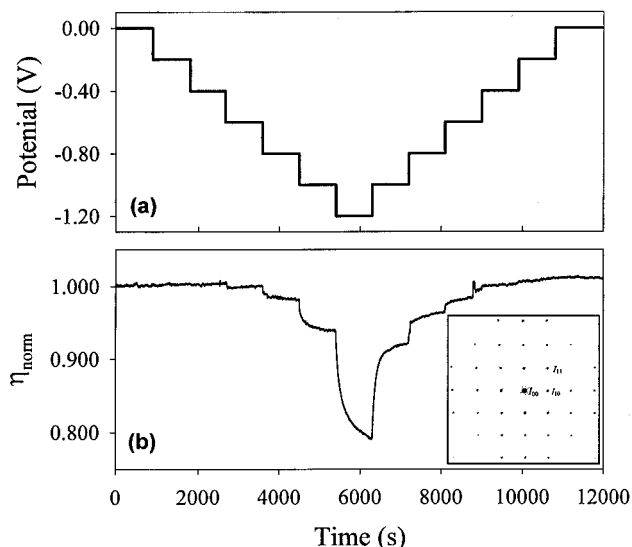


Figure 2. Potential dependent diffraction of a micropatterned nanocrystalline TiO_2 film in 1 M LiClO_4 /propylene carbonate. (a) Applied potential as function of time. (b) Normalized diffraction efficiency as a function of time. Inset: Experimental diffraction pattern.

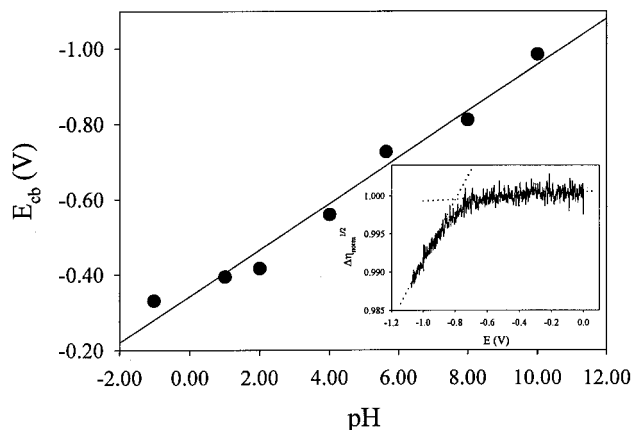


Figure 3. Dependence of diffraction-derived conduction-band-edge energy on the pH value of the solution. Inset: A plot of $\Delta\eta_{\text{norm}}^{1/2}$ of nanostructured TiO_2 as a function of applied potential in an aqueous solution (pH 8.00). η_{norm} is the diffraction efficiency normalized to 1 at the beginning of the scan.

(More negative values have been observed, however, in rigorously dried propylene carbonate solutions.¹⁹) The coincidence of the potentials is qualitatively consistent with the expectation that addition of electrons to the semiconductor (possible at potentials equal to or more negative than E_{cb}) will alter the electronic polarizability of the semiconductor, thereby changing the refractive index and changing the diffraction efficiency, an idea we consider in further detail below. We note further that electrochemical modulation of diffraction of visible light has previously been reported for other types of electrode materials or films.²⁰

Potential-modulated diffraction in aqueous solutions.—The conduction-band-edge energy is somewhat better defined (or at least, somewhat easier to control experimentally) in aqueous environments. Furthermore, E_{cb} is known to shift in an approximately Nernstian behavior with pH; in one recent report E_{cb} for nanocrystalline anatase thin-film electrodes was $0.36\text{-}0.06 \text{ V}$ per pH unit (vs. Ag/AgCl).²¹ We reasoned that similar experiments here would offer an instructive test of the applicability of the proposed diffraction approach. Figure 3 shows results from a series of variable-pH dif-

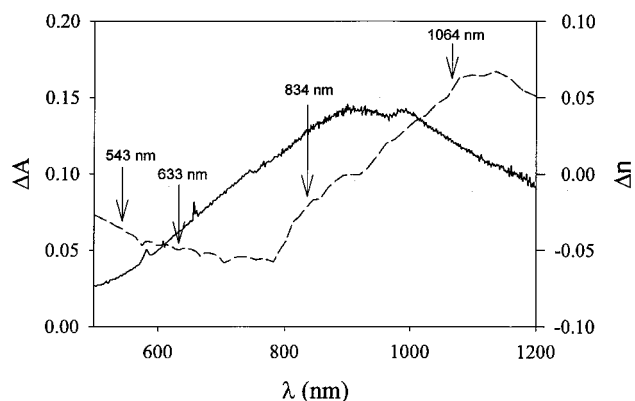


Figure 4. The solid line with axis on the left is the optical absorption spectrum of an anatase TiO₂ electrode measured at 1 M LiClO₄ propylene carbonate solution following polarization for 10 min at -1.2 V. The spectrum measured after stabilization for 10 min at 0.0 V has been subtracted. The dashed line with axis on the right shows the variation in Δn with wavelength predicted by Eq. 3.

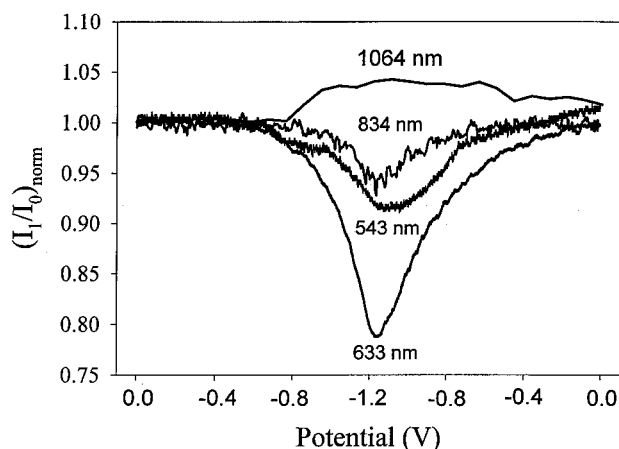


Figure 5. Data from the study of electrochemically modulated diffraction efficiency for TiO₂ in the potential scanning experiments. The wavelength of the diffracting light was 543, 633, 834, or 1064 nm. Scan rate was 1 mV/s (for 543, 633, and 834 nm) or 100 mV/s (for 1064 nm). Electrolyte was 1 M LiClO₄ in propylene carbonate.

fraction experiments. Plotted are onset potentials for diminution in diffraction efficiency at $\lambda = 633$ nm based on voltammetric scans at 1 mV/s. [Shown as an inset is a plot of the square root of the normalized diffraction efficiency (η_{norm}) vs. potential in a representative solution. As shown by the plot, the definition of onset potential is somewhat ambiguous. We chose to define the potential as the intersection point of two tangents drawn to the linear parts of the curve.] The measurements clearly show the expected dependence of E_{cb} on pH. A best-fit straight line gives $E_{\text{cb}} = -0.34 - 0.061$ V per pH unit.

Potential-modulated diffraction: Incident wavelength effects.— To account for the observed dependence of the diffraction efficiency on the applied potential, the underlying factors affecting the diffraction efficiency must be considered. It is known that the diffraction efficiency of a grating depends on the optical properties of the grating material, especially the absorptivity or imaginary component of the refractive index, k , and the real component of the refractive index, n . An expression that is quantitatively applicable for first-order diffraction by thin, l -dimensional sinusoidal gratings (admittedly, not quite the case here) is the following²²

$$\eta(\lambda) = \exp[-2.3OD(\lambda)/\cos\theta](\pi d/\lambda\cos\theta)\{\Delta k(\lambda)^2 + \Delta n(\lambda)^2\} \quad [2]$$

where $OD(\lambda)$ is the average optical density (absorbance and scattering losses) of the grating at wavelength λ , d is the grating thickness, and θ is the Bragg angle. $\Delta k(\lambda)$ and $\Delta n(\lambda)$ are, respectively, the difference in the peak and null values of k and n at wavelength λ . In our experiments, $\Delta k(\lambda)$ and $\Delta n(\lambda)$ correspond to the difference in the absorptivity and refractive index of TiO₂ and electrolyte solution at wavelength λ . In addition to a leading term accounting for absorption losses, the expression indicates that the (first-order) diffraction efficiency is proportional to the square of the refractive index and absorptivity contrast terms. The equation further implies that to observe changes in diffraction efficiency, the applied electrode potential must provide changes in one or several optical or structural parameters. We assume at the outset that changes in the film thickness, d , can be neglected, although clearly this will not be the case for all electrode materials. Changes in the imaginary portion of the refractive index and in the film's optical density require an electrochemical change in the electronic absorption spectrum. The electrochemical addition of electrons to near-band-edge trap sites is known to induce a broad electronic transition or transitions in the red and near-infrared regions of the spectrum. The transition has been variously ascribed to a forbidden Ti(III) d-d transition and to an allowed Ti(III)-oxo-Ti(IV) intervalence transition.¹⁴ In any case, Fig. 4 shows that a detectable absorption feature, with a maximum at 900 nm, can be generated by balancing the titanium dioxide electrode (in this case, an unpatterned electrode) at a potential negative of the conduction band edge.

The introduction of a new electronic transition can also affect the real portion of the refractive index. Furthermore, n can be influenced even at wavelengths significantly removed from the transition. The expected relationship between n and k is given by the following form of the Kramers-Kronig expression²³

$$\Delta n(\omega') = \frac{c}{\pi} \int_0^{\infty} \frac{\Delta\alpha(\omega)}{\omega^2 - \omega'^2} d\omega \quad [3]$$

where $\Delta\alpha$ is the wavelength or frequency dependent change in absorption coefficient where $\alpha = 4\pi k/\lambda$, ω is $2\pi c/\lambda$, and ω' is the optical frequency of interest for Δn evaluation. Qualitatively, the equation predicts an increase in n at incident wavelengths longer than that for the absorption maximum, λ_{max} , upon introduction of a new absorption band. It also predicts a decrease in n at incident wavelengths shorter than λ_{max} . The dashed line in Fig. 4 shows the relative variation in Δn with wavelength predicted by Eq. 3. Measurements made at $\lambda = 633$ nm (for example, Fig. 2 and 3) show a decrease in diffraction efficiency concomitant with the change in optical density. This behavior could conceivably reflect both absorption losses (ΔOD term) and overall refractive index ($n + ik$) attenuation. The former is of less interest to us. To remove it from the evaluation of diffraction effects, we chose to recast the findings in terms of relative diffraction proportions, I_{10}/I_{00} , where I_{10} is the intensity of diffracted light at the 1,0 spot in the diffraction pattern and I_{00} is the intensity of light at the 0,0 spot, *i.e.*, the intensity of the transmitted light that remains undiffracted. Note that absorption losses attenuate I_{10} and I_{00} in proportionately equal fashion, thereby leaving the ratio unaffected by the losses.

With this analysis and the Kramers-Kronig expression in mind, I_{10}/I_{00} or I_{11}/I_{00} was measured as a function of potential at 543, 633, 834, and 1064 nm. As shown in Fig. 5, at potentials negative of E_{cb} the ratio decreases for $\lambda = 543, 633,$ and 834 nm, with the greatest decrease occurring at $\lambda = 633$ nm. These observations are consistent with an electrochemically induced decrease in Δn and with a greater role for Δn than Δk in determining the diffraction efficiency (see Eq. 3). (Notice that at $\lambda = 543$ nm, ΔOD is essentially zero and therefore, Δk is essentially zero, leaving only the real component of the refractive index to be modulated.) At $\lambda = 1064$ nm, on the other hand,

I_{11}/I_{00} increases, as expected if Δn exhibits the increase as promised by the Kramers-Kronig relation.

The greater sensitivity of the normalized diffraction ratio to variations in the real component of the refractive index than to variations in the absorptivity suggests that the diffraction methodology might prove particularly advantageous when exceptionally thin semiconductor film electrodes are examined (*i.e.*, electrodes displaying very little change in optical density). Presumably, related techniques such as electrochemically induced probe beam deflection²⁴ would offer similar sensitivity advantages. The diffraction approach might also prove advantageous when only off-resonance (nonabsorbing) optical probing is possible. Note that Eq. 3 predicts changes in n even at wavelengths where a film is nonabsorbing.

Conclusions

Micropatterned titanium dioxide thin-film electrodes exhibit efficient diffraction in the presence of aqueous or nonaqueous electrolyte solutions. The diffraction efficiency can be modulated electrochemically. At the wavelengths examined, the modulation is caused by changes in both real and imaginary components of the refractive index. The index changes, in turn, are caused by the addition of electrons to near-band-edge trap sites and by optical absorption by the trapped electrons. The onset potential for diffraction modulation provides a good measure of the potential of the electrode's conduction bandedge. Variable excitation wavelength measurements show that, after correction for absorption losses, the electrochemically induced changes in the proportion of light diffracted can be either positive or negative. The signs and the relative magnitudes of the wavelength-dependent changes are well described by a Kramers-Kronig analysis that assumes that changes in the real component of the refractive index dominate the response.

Acknowledgments

We gratefully acknowledge Dr. K. Stevenson and Dr. G. Mines for helpful discussions. We thank the Office of Naval Research and the Northwestern University Institute for Environmental Catalysis for financial support.

Northwestern University assisted in meeting the publication costs of this article.

References

1. B. O'Regan and M. Grätzel, *Nature*, **353**, 737 (1991).
2. A. Hagfeld and M. Grätzel, *Chem. Rev.*, **95**, 49 (1995).
3. L. Sopyan, S. Murasawa, K. Hashimoto, and A. Fujishima, *Chem. Lett.*, 723 (1994).
4. A. Wold, *Chem. Mater.*, **5**, 280 (1993).
5. T. Ohzuku and T. Hirai, *Electrochim. Acta.*, **27**, 1263 (1982).
6. T. Ohzuku, Z. Takehara, and S. Yoshizawa, *Electrochim. Acta.*, **24**, 219 (1979).
7. See, for example, F. Cao, G. Oskam, P. C. Searson, J. M. Stipkala, T. A. Heimer, F. Farzad, and G. J. Meyer, *J. Phys. Chem.*, **99**, 11974 (1995).
8. (a) W. J. Albery and P. N. Bartlett, *J. Electrochem. Soc.*, **131**, 315 (1984); (b) G. Hodes, I. D. J. Howell, and L. M. Peter, *J. Electrochem. Soc.*, **139**, 3136 (1992).
9. (a) G. Boschloo and D. Fitzmaurice, *J. Phys. Chem. B*, **103**, 3093 (1999); (b) G. Rothenberger, D. Fitzmaurice, and M. Grätzel, *J. Phys. Chem.*, **96**, 5983 (1992); (c) G. Redmond and D. Fitzmaurice, *J. Phys. Chem.*, **97**, 1426 (1993).
10. L. A. Lyon and J. T. Hupp, *J. Phys. Chem.*, **99**, 15718 (1995).
11. L. A. Lyon and J. T. Hupp, *J. Phys. Chem. B*, **103**, 4623 (1999).
12. (a) B. I. Lemon and J. T. Hupp, *J. Phys. Chem. B*, **103**, 3797 (1999); (b) B. I. Lemon, Ph.D. Thesis, Northwestern University, Evanston, IL (1999).
13. P. Krtil, L. Kavan, and D. Fattakhova, *J. Solid State Electrochem.*, **1**, 83 (1997).
14. B. I. Lemon, L. A. Lyon, and J. T. Hupp, in *Nanoparticles in Solids and Solutions. Preparation, Characterization and Applications*, J. H. Fendler, Editor, VCH-Wiley, New York (1998).
15. K. J. Stevenson, G. J. Hurrst, and J. T. Hupp, *Electrochem. Solid-State Lett.*, **2**, 175 (1999).
16. L. Kavan, B. O'Regan, A. Kay, and M. Grätzel, *J. Electroanal. Chem.*, **346**, 291 (1993).
17. C. H. Rochester, *Acidity Functions*, Academic Press, New York (1970).
18. L. Kavan, M. Grätzel, J. Rathouský, and A. Zukal, *J. Electrochem. Soc.*, **143**, 394 (1996).
19. B. Enright, G. Redmond, and D. Fitzmaurice, *J. Phys. Chem.*, **98**, 6195 (1994).
20. (a) T. S. Bergstedt, B. T. Hauser, and K. S. Schanze, *J. Am. Chem. Soc.*, **116**, 8380 (1994); (b) K. S. Schanze, T. S. Bergstedt, and B. T. Hauser, *Adv. Mater.*, **8**, 531 (1996); (c) F. Nakajima, Y. Hirakawa, T. Kaneta, and T. Imasaka, *Anal. Chem.*, **71**, 2262 (1999); (d) A. B. Bocarsly, C. C. Chang, Y. Wu, and E. P. Vicenzi, *J. Chem. Ed.*, **74**, 663 (1997); (e) K. S. Schanze, T. S. Bergstedt, B. T. Hauser, and C. S. P. Cavalheiro, *Langmuir*, **16**, 795 (2000).
21. G. Boschloo and D. Fitzmaurice, *J. Phys. Chem. B*, **103**, 7860 (1999).
22. K. A. Nelson, R. Casalegno, R. J. D. Miller, and M. D. Fayer, *J. Chem. Phys.*, **77**, 1144 (1982).
23. G. R. Olbright and N. Peyghambarian, *Appl. Phys. Lett.*, **48**, 1184 (1986).
24. M. Vilas-Boas, M. J. Henderson, C. Freire, and A. R. Hillman, *Chem. Eur. J.*, **6**, 1160 (2000).